

Computational Techniques for Conservation Law PDEs

Ruochen Zhao

ruochen.zhao16@imperial.ac.uk

Abstract

This is an overview of the project undertaken during my UROP stay at the Complex Multiscale System group, led by Professor Serafim Kalliadasis. In my study, four numerical methods are investigated, which are finite volume method, finite difference method, Monte Carlo method and molecular dynamics, where the first two are implemented to solve various equations in fluid dynamics and the last two are used to simulate the hard sphere system.

1 Finite Difference Method

1.1 Method

The finite difference can be formulated in various ways. Consider the Taylor's series of an arbitrary function

$$f(x + \Delta x) = f(x) + \frac{f'(x)}{1!} \Delta x + \frac{f''(x)}{2!} \Delta x^2 + \frac{f'''(x)}{3!} \Delta x^3 + \dots$$

Solve for $f'(x)$

$$f'(x) = \frac{f(x + \Delta x) - f(x)}{\Delta x} + \mathcal{O}(\Delta x)$$

One can approximate by removing $\mathcal{O}(\Delta x)$, namely the truncating error

$$f'(x) \approx \frac{f(x + \Delta x) - f(x)}{\Delta x}$$

The formula above is the essence of finite difference. Higher derivatives can be obtained by taking the finite difference of the lower derivatives.

1.2 Example

Consider the heat equation

$$\frac{\partial u}{\partial t} = \alpha \frac{\partial^2 u}{\partial x^2}$$

The equation can be discretised using the finite difference. Different ways of discretisation are possible, a central difference method is shown below

$$\frac{u_i^{n+1} - u_i^n}{\Delta t} = \alpha \frac{u_{i+1}^n - 2u_i^n + u_{i-1}^n}{(\Delta x)^2}$$

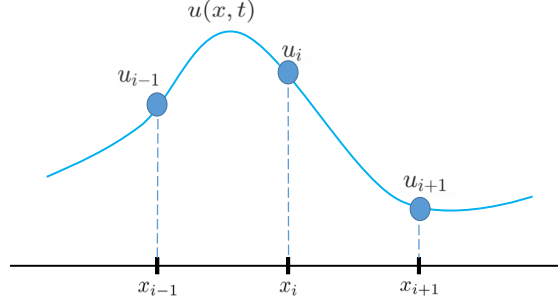


Figure 1: Discretisation of the function

Given the initial and boundary conditions $u(x, 0) = 0$, $u(0, t) = 80$ and $u(0.1, t) = 40$, the equation can be solved numerically.

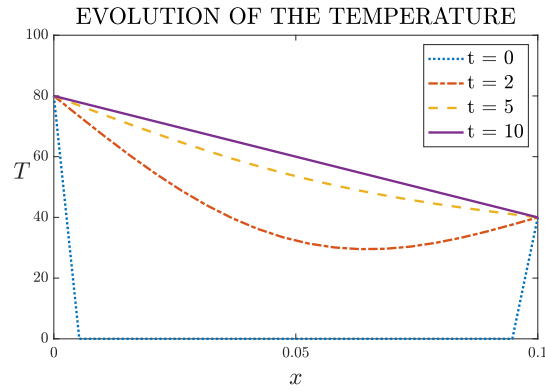


Figure 2: Numerical solution of the heat equation

The temperature converges to a linear profile, which is exactly the analytical solution of the heat equation.

1.3 Properties

1.3.1 The CFL Condition

In the example above no restriction is mentioned on the choice of Δx or Δt . In fact these choices are constrained. For a linear, well-posed PDE, the numerical scheme converges if

1. It is consistent, i.e. $\lim_{\Delta x, \Delta t \rightarrow 0} \text{Truncating Error} = 0$
2. and stable, i.e. $\left| \frac{u_i^{n+1}}{u_i^n} \right| \leq 1$

The CFL condition for the heat equation is established by applying a von Neumann analysis to the second requirement, which has the form $\frac{\lambda_{max} \Delta t}{\Delta x} \leq 1$. It will vary for different equations. Its physical meaning is that the numerical regime has to cover the physical propagation of information.

1.3.2 Explicit and Implicit Methods

The method used above is an explicit one, where u_i^{n+1} is obtained directly from $u_{i-1}^n, u_i^n, u_{i+1}^n$. Implicit methods are possible too, where u_i^{n+1} is expressed in terms of both known and unknown quantities at time n and $n+1$ and is obtained by solving a system of algebraic equations. It requires more computation power but allows larger Δt . The choice of explicit and implicit methods should be best suited to the actual problems.

2 Finite Volume Method

2.1 Method

Finite volume is inherently similar to finite difference, i.e. the properties of FD apply to FV as well. Instead of using points, cells which have a finite volume are used. Consider the advection equation

$$\frac{\partial \rho}{\partial t} + c \frac{\partial \rho}{\partial x} = s(x)$$

Compute the cell averages for all i , defined as

$$\bar{\rho}_i = \frac{1}{\Delta x} \int_{x_{i-1/2}}^{x_{i+1/2}} \rho(x) dx$$

Reconstruct the values in each cell from cell averages. Different reconstruction orders are possible: piece-wise constant, linear, quadratic, etc.

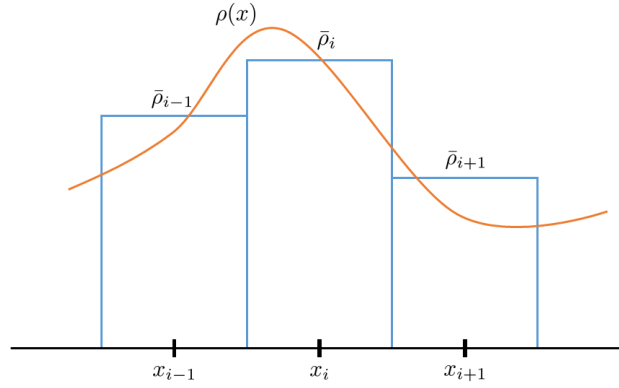


Figure 3: Linear reconstruction of the function

Consider fluxes at the cell boundaries, i.e. $F_{i-1/2}, F_{i+1/2}$, in this case $F(\rho) = c\rho$. Apply divergence theorem at the boundaries and discretise the equation

$$\frac{\bar{\rho}_i^{n+1} - \bar{\rho}_i^n}{\Delta t} = - \frac{F_{i+1/2}^n - F_{i-1/2}^n}{\Delta x} + s_i^n$$

Compute the fluxes by numerical flux functions

$$F_{i+1/2}(\rho) = \tilde{F}(\rho_1, \dots, \rho_i, \rho_{i+1}, \dots, \rho_n)$$

At steady state, analytically $\partial_x F = s(x)$, but this may not be true numerically, i.e. the flux and the source may not be exactly balanced.

2.2 Example

2.2.1 The Advection Equation

$$\frac{\partial \rho}{\partial t} + c \frac{\partial \rho}{\partial x} = 0$$

The analytical solution of this equation is the d'Alembert's solution, i.e. wave propagating at constant velocity. A backward method is used in the numerical solution. See Fig. 4a.

2.2.2 The Burgers Equation

$$\frac{\partial \rho}{\partial t} + \rho \frac{\partial \rho}{\partial x} = v \frac{\partial^2 \rho}{\partial x^2}$$

This equation is a combination of the heat equation (aka the diffusion equation) and the advection equation, therefore a combined effect should be observed, i.e. diffusion and advection occurring simultaneously. Note the wave velocity is no longer a constant and the nonlinear term $\rho \partial_x \rho$ will introduce discontinuity in the solution, known as shock waves. An upwind method is used in the numerical solution. See Fig. 4b.

2.2.3 The Euler Equation

$$\begin{cases} \partial_t \rho + \partial_x (\rho u) = 0 \\ \partial_t (\rho u) + \partial_x (\rho u^2 + p) = -\rho \partial_x \frac{x^2}{2} \end{cases}$$

This equation conserves both mass and momentum and there is an external pressure of $\frac{x^2}{2}$. The analytical solution can be readily obtained by setting all time derivatives to zero and solving the remaining ODE. The final density profile should have a Gaussian shape and the momentum should not change from the initial condition. A local Lax-Friedrich method is used in the numerical solution. See Fig. 4c.

2.2.4 The Gradient Flow Equation

$$\partial_t \rho = \partial_x (\rho \partial_x (\rho + \frac{x^4}{4} - \frac{x^2}{2}))$$

This equation is proposed in the paper by Carrillo, Chertock and Huang.¹ It can be derived from the Euler equations by applying the overdamped limit, i.e. $\partial_x \rho u^2 \approx 0$. The difference is that now the pressure is ρ^2 , i.e. isentropic gases, whereas in the Euler equations it is ρ , i.e. ideal gases. The fact that the pressure is not proportional to the density will result vacuum in the solution. Moreover, the external potential is now double-welled, which means two peaks will be present. If an initial condition that is a Gaussian distribution slightly shifted to one side is used, one peak will have a higher mass than the other, because initially more mass is located on one side. If the wells are deep enough to accommodate larger masses (the depth is linked to the coefficients of the potential), this resulting peaks will have equal masses. See Fig. 4d.

¹J.A. Carrillo, A. Chertock and Y. Huang, Commun. Comput. Phys. **17**, 1, 233–258 (2015)

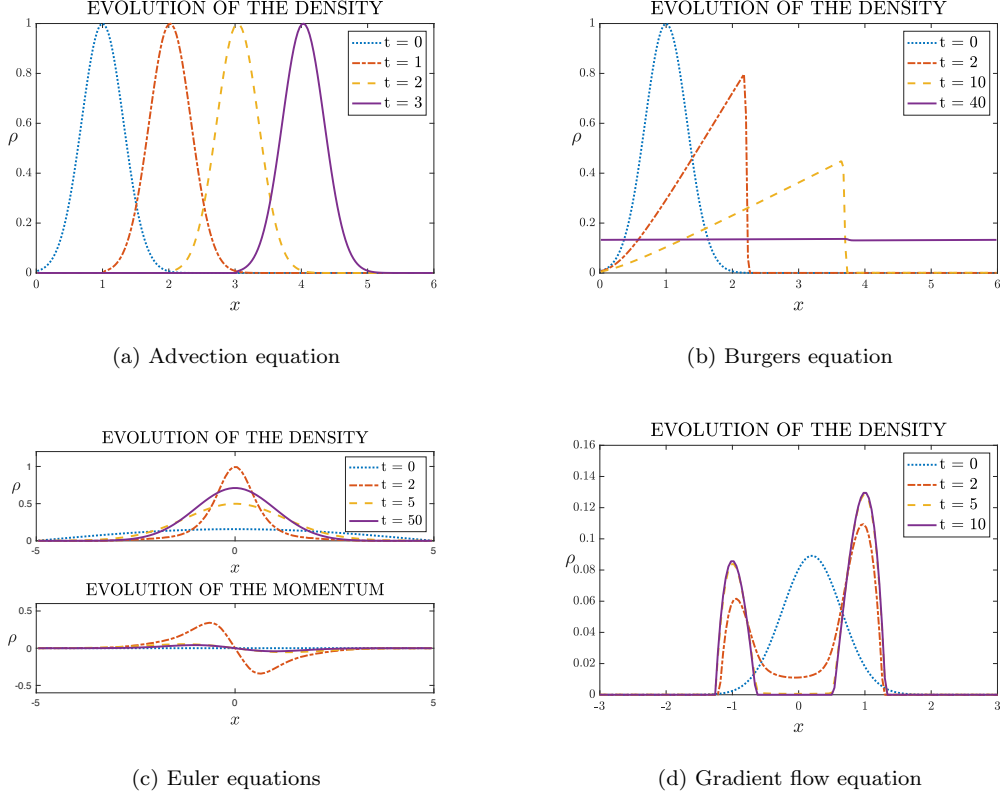


Figure 4: Numerical solutions of the equations

3 Monte Carlo Method

3.1 The Hard Sphere Model

Hard spheres are model particles used widely in the statistical mechanics of fluids and solids, they never overlap and are defined in terms of potentials:

$$V(\mathbf{r}_1, \mathbf{r}_2) = \begin{cases} 0 & \text{if } |\mathbf{r}_1 - \mathbf{r}_2| \geq \sigma \\ \infty & \text{if } |\mathbf{r}_1 - \mathbf{r}_2| < \sigma \end{cases}$$

where \mathbf{r}_1 and \mathbf{r}_2 are the positions of particles and σ is the diameter of particles

The objective is to investigate the evolution of density of the hard spheres in a 1-D box under an external potential of x^2 .

3.2 Method

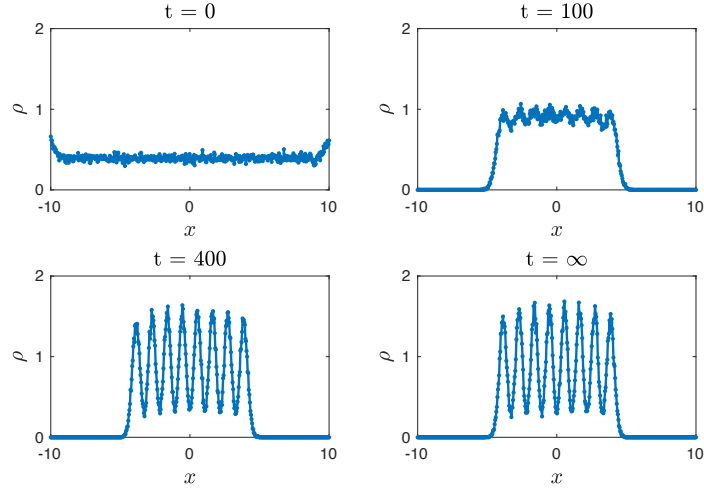
The Monte Carlo algorithms exploit randomness to solve problems that may be deterministic in nature but difficult to solve analytically. One variation is the Metropolis algorithm, which has the following steps:

1. Set an initial configuration C_i , where $i = 0$
2. Randomly generate a new state C_j from the current configuration

3. Compute the potential change between the two states, i.e. $U_j - U_i$
4. Accept the new state with a probability of $\exp(-(U_j - U_i))$
5. Increase i by 1 and return to step 2

For the hard sphere example, initially eight particles are randomly distributed and the new states are generated from moving each particle for a random distance. The relation between the time step and the moved distance is derived from kinetic theory and we take $\Delta x = \Delta t \cdot \mathcal{N}(0, 1)$ in this case.

3.3 Result



This result agrees well with theory. The eight peaks represent the eight particles, which are separated at a distance comparable to their diameter, due to repulsions. The peaks are concentrated in the middle and this is caused by the external potential, which has an upward parabola shape and attracts particles to the center. The area under the peaks are equal to the total mass of the particles, meaning mass is conserved during the evolution.

4 Molecular Dynamics

4.1 Method

Unlike in Monte Carlo where a fixed recipe is conceived for the particles to generate new states, in MD the new states are determined by the integration of Newton's equations of motion. For instance, the Velocity Verlet method:

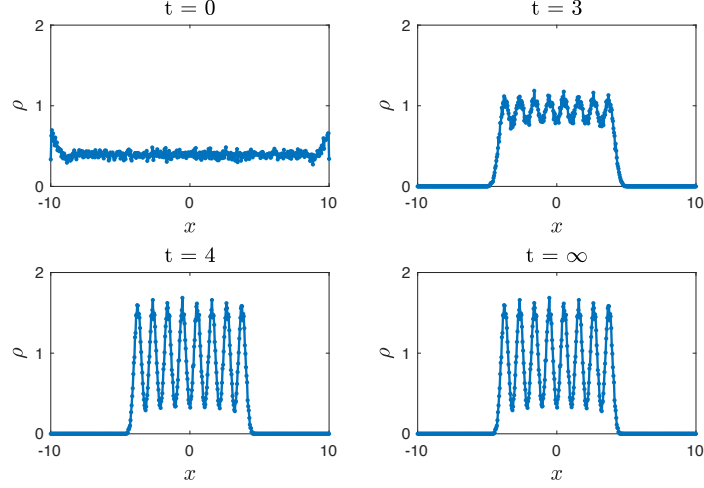
$$\begin{cases} \vec{x}(t + \Delta t) = \vec{x}(t) + \vec{v}(t)\Delta t + \frac{\vec{F}(t)}{2m}\Delta t^2 \\ \vec{v}(t + \Delta t) = \vec{v}(t) + \frac{\vec{F}(t) + \vec{F}(t + \Delta t)}{2m}\Delta t \end{cases}$$

For the hard sphere model, since $\vec{F}(t) = -\nabla V$, instead the WCA potential which is continuous is used:

$$V(r) = 4[(\frac{\sigma}{r})^{12} - (\frac{\sigma}{r})^6] \quad \text{for } r < 2^{1/6}\sigma$$

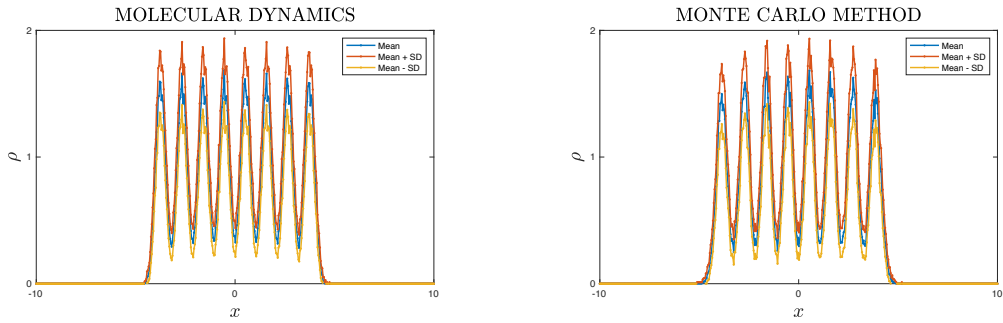
where r is the distance between particles and σ is the diameter of particles

4.2 Result



This result is similar to that of the MC. They differ in that MC requires much longer time to reach equilibrium distribution. One possible reason is that, as mentioned before, it is unclear how the discrete jumps in MC are related to the time step and more rigorous physical arguments are necessary. Another fact is that MD is deterministic, whereas MC is a stochastic process, meaning it is possible that the particles jump against the external potential. Those 'upwind' jumps slow down the system from evolving towards the equilibrium.

4.3 Comparison between MC and MD



The figure above shows the average density profile, as well as the profiles within one standard deviation, which can be considered as the error range of the methods. Both methods show very similar ranges, thus it can be concluded that they are close in accuracy for this system.